Table 5. Experiment 2; body and organ weights, and leucocyte typing and counting of dams

Items	MWCNT dose (mg/kg body weight)			
	0 (control)	3	4	5
Number of dam	10	10	15	5
Body weight on day 9 of the gestation	33.0 ± 2.0	33.6 ± 2.8	33.8 ± 2.8	32.5 ± 2.2
on day 18 of the gestation	55.4 ± 3.1	58.4 ± 5.5	59.1 ± 6.9	45.1 ± 4.5*
Organ weight				
Liver (g)	2.80 ± 0.27	2.73 ± 0.36	3.05 ± 0.31	2.44 ± 0.11
Kidney (mg)	454 ± 52	431 ± 60	457 ± 54	422 ± 28
Heart (mg)	155 ± 10	161 ± 14	162 ± 15	150 ± 9
Lung (mg)	157 ± 14	168 ± 10	197 ± 51	228 ± 47**
Spleen (mg)	136 ± 22	122 ± 29	149 ± 40	158 ± 35
Thymus (mg)	19.9 ± 7.5	16.4 ± 5.3	18.9 ± 5.5	13.9 ± 8.9
Tracheobronchial lymph node (mg)	4.2 ± 3.6	6.8 ± 5.2	6.2 ± 4.3	8.7 ± 2.3
Leucocyte count ($10^2/\mu l$)				
Total	37.5 ± 6.4	49.5 ± 11.3	51.6 ± 11.5*	51.3 ± 10.6*
Lymphocyte	21.0 ± 4.4	30.0 ± 8.2	26.5 ± 7.4	22.5 ± 6.4
Neutrophil	14.7 ± 4.5	17.4 ± 9.7	20.3 ± 11.2	25.4 ± 11.5
Eosinophil	0.7 ± 0.9	1.1 ± 0.7	2.7 ± 2.5	1.6 ± 1.1
Monocyte	1.2 ± 0.7	1.0 ± 0.5	2.2 ± 1.4	1.7 ± 0.4

Values are the means ± S.D. Asterisks represent that values are significantly different from the control value (* or ** indicating $p < 0.05$ or 0.01, respectively).

Table 6. Experiment 2; incidences of malformations

Items	MWCNT dose (mg/kg body weight)			
	0 (control)	3	4	5
External malformation				
Number of litters with malformed fetuses/examined (percentages in the parentheses)				
	0/10(0)	0/10(0)	5/14(35.7)*	2/5(40.0)*
Percent incidence of malformations#	0	0	15.6 ± 27.9	5.6 ± 8.2
Number of malformed fetuses/examined	0/113	0/133	15/158***	3/44**
Number of fetuses with				
short or absent tail	0	0	12**	3**
reduction deformity of limb	0	0	7*	0
Skeletal malformation				
Number of litters with malformed fetuses/examined (percentages in the parentheses)				
	0/10(0)	1/10(10.0)	6/14(42.8)*	4/5(80.0)*
Percent incidence of malformations#	0	0	39.9 ± 48.4*	61.9 ± 38.2*
Number of malformed fetuses/examined	0/113	1/133	56/158***	31/44***
Number of fetuses with				
fusion of ribs	0	0	8*	10***
fusion of vertebral bodies and arches	0	0	54***	25***
hypophalangia	0	0	10*	1
hyperphalangia	0	1	0	1

Calculated by averaging the percentage in each litter (*i.e.*, number of malformations/fetuses) and shown as the means ± S.D. Asterisks represent that the values are significantly different from the control value (*, ** or *** indicating $p < 0.05$, 0.01 or 0.001, respectively).

exposure situation of the inhalation. The highest dose of 5 mg/kg body weight must have been too high, because it caused the apparent maternal toxicity, and it agglomerated in the lung (data not shown). It is clearly indicated, however, that MWCNT is teratogenic, because the malformations in the fetuses were significantly induced by the middle dose of 4 mg/kg body weight that did not cause the apparent maternal toxicity.

It is known that methyl cellulose of a certain length has nephrotoxicity but, in this study, no adverse effect on kidney of dam given 2% CMCNa solution (control) nor suspension of MWCNT in 2% CMCNa (dosed groups) was observed.

Mechanisms underlying the teratogenicity of MWCNT are still obscure. Sargent *et al.* (2009) has demonstrated that single-wall carbon nanotube induces aneuploidy in cultures primary and immortalized human airway epitherial cells by the disruption of the mitotic spindle. In that study, the association of nanotubes with cellular and mitotic tubulins as well as chromatins within the nuclei is demonstrated, and the similarity of nanotube bundles to microtubules in size of microtubules is considered to play roles, because it may make nanotubes incorporated into the mitotic spindle apparatus. Recently, Takahashi *et al.* (2010) has reported that MWCNT also induces polyploidy, suggesting that MWCNT may exert similar effects on microtubules to the situation of single-wall carbon nanotube. If it is a case, the disruption of the mitotic spindle and the fragmentation of the centrosomes may inhibit subsequent cell division, which results in the embryonic death in early phase and the malformation of the reduction type. Further studies are apparently warranted, and especially a passage of MWCNT through the placenta and the reach to the fetus should be evidenced.

Another possible factor involved in the teratogenicity may be the chronically persisting inflammation caused by the exposure to MWCNT, which is frequently considered to participate in the biological effects of nanomaterials (Takagi *et al.*, 2008; Sakamoto *et al.*, 2009; Erdely *et al.*, 2009; Hubbs *et al.*, 2011). The present results of the increments of the numbers of leucocyte and related hemocytes, and of the weight of the spleen might support this possibility.

The present intratracheal study gives no-observed-adverse-effect level (NOAEL) of 3 mg/kg body weight for external and skeletal malformations. Although the human exposure level of MWCNT has not as yet clearly determined, the interim report for the risk assessment of MWCNT by the National Institute of Advanced Industrial Science and Technology (AIST, 2009) roughly estimated the quantity of MWCNT exposure of workers as 0.53- 6.20 μg/kg/day. Comparing with these values, the above NOAEL for external and skeletal malformations are approximately 480-5,660 times high. It is thus tentatively evaluated that the present results may not necessarily or immediately indicate a human risk. Needless to say, however, more detailed and careful investigations including those for the teratogenicity must be conducted to complete the risk assessment of MWCNT.

ACKNOWLEDGMENTS

This work was supported in part by a research budget of the Tokyo Metropolitan Government, Japan, and a Grant-in-Aid from the Ministry of Health, Labor and Welfare of Japan. Authors gratefully thank to Mr. Ando, Mr. Kubo, Mr. Yano, Mr. Takahashi, Mr. Yuzawa and Mr. Nagasawa, for their technical assistance.

REFERENCES

Dawson, A.B. (1926): A note on the staining of the skeleton of cleared specimens with Alizarin Red S. Stain Techno., **1**, 123-124.

Erdely, A., Hulderman, T., Salmen, R., Liston, A., Zeidler-Erdely, P.C., Schwegler-Berry, D., Castranova, V., Koyama, S., Kim, Y.-A., Endo, M. and Simeonova, P.P. (2009): Cross-talk between lung and systemic circulation during carbon nanotube respiratory exposure. Potential biomarkers. Nano Letters, **9**, 36-43.

Hubbs, A.F., Mercer, R.R., Benkovic, S.A., Harkema, J., Sriram, K., Schwegler-Berry, D., Goravanahally, M.P., Nurkiewicz, T.R., Castranova, V. and Sargent, L.M. (2011): Nanotoxicology--A pathologist's Perspective. Toxicol. Pathol., **39**, 301-324.

Kameyama, Y., Tanimura, T. and Yasuda, M. (1980): Spontaneous malformations in laboratory animals : Photographic atlas and reference data. Congenital Anomalies, **20**, 25-106. (in Japanese).

Lam, C.-W., James, J.T., McCluskey, R., Arepalli, S. and Hunter, R.L. (2006): A review of carbon nanotube toxicity and assessment of potential occupational and environmental health risks. Crit. Rev. Toxicol., **36**, 189-217.

Martin, C.R. and Kohli, P. (2003): The emerging field of nanotube biotechnology. Nat. Rev. Drug Discov., **2**, 29-37.

National Institute of Advanced Industrial Science and Technology (AIST) (2009): The interim report--the risk assessment of nanomaterials (CNT)--Executive summary. (in Japanese).

Nishimura, H. (1976): Could skin applications of cleaning detergents be teratogenic? Course of the successive joint studies and interpretation of the results. Congenital Anomalies, **16**, 175-185. (in Japanese).

Ogata, A., Ando, H., Kubo, Y. and Hiraga, K. (1984): Teratogenicity of thiabendazole in ICR mice. Food Chem. Toxicol., **22**, 509-520.

Ogata, A., Yoneyama, M., Sasaki, M., Suzuki, K. and Imamichi, T. (1987): Effects of pretreatment with SKF-525A or sodium phenobarbital on thiabendazole-induced teratogenicity in ICR mice. Food Chem. Toxicol., **25**, 119-124.

Ogata, A., Fujitani, T., Yoneyama, M., Sasaki, M. and Suzuki, K. (1989): Glutathione and cysteine enhance and diethylmaleate reduces thiabendazole teratogenicity in mice. Food Chem.

Toxicol., **27**, 117-123.

Ogata, A., Ando, H., Kubo, Y., Nagasawa, A., Ogawa, H., Yasuda, K. and Aoki, N. (1999): Teratogenicity of thujaplicin in ICR mice. Food Chem. Toxicol., **37**, 1097-1104. Erratum in Food Chem. Toxicol., 2000, **38**, 125.

Pacurari, M., Castranova, V. and Vallyathan, V. (2010): Single- and multi-wall carbon nanotubes versus asbestos: Are the carbon nanotubes a new health risk to humans? J. Toxicol. Environ. Health Part A, **73**, 378-395.

Sakamoto,Y., Nakae, D., Fukumori, N., Tayama, K., Maekawa, A., Imai, K., Hirose, A., Nishimura, T., Ohashi, N. and Ogata, A.(2009): Induction of mesothelioma by a single intrascrotal administration of multi-wall carbon nanotube in intact male Fischer 344 rats. J. Toxicol. Sci., **34**, 65-76.

Sargent, L.M., Shvedova, A.A., Hubbs, A.F., Salisbury, J.L., Benkovic, S.A., Kashon, M.L., Lowry, D.T., Murray, A.R., Kisin, E.R., Friend, S., McKinstry, K.T., Battelli, L. and Reynolds, S.H. (2009): Induction of aneuploidy by single-walled carbon nanotubes. Environ. Mol. Mutagen., **50**, 708-717.

Scott, N.R. (2005): Nanotechnology and animal health. Rev. Sci. Tech., **24**, 425-432.

Takagi, A., Hirose, A., Nishimura, T., Fukumori, N., Ogata, A., Ohashi, N., Kitajima, S. and Kanno, J. (2008): Induction of mesothelioma in p53+/- mouse by intraperitoneal application of multi-wall carbon nanotube. J. Toxicol. Sci., **33**, 105-116.

Takahashi, T., Asada, S., Hara, T., Toyoizumi, T., Saitoh, Y., Kumagai, H., Yamakage, K. and Honma, M (2010): Chromosomal aberration test of multi-wall carbon nanotubes (MWCNT) using CHL/IU cells. 39th Annual Meeting of the Japanese Environmental Mutagen Society, Program abstract.

The Journal of Toxicological Sciences (J. Toxicol. Sci.)
Vol.37, No.1, 177-189, 2012

Original Article

Effects of sustained stimulation with multi-wall carbon nanotubes on immune and inflammatory responses in mice

Atsumi Yamaguchi[1], Tomoko Fujitani[1], Ken-ichi Ohyama[1], Dai Nakae[2], Akihiko Hirose[3], Tetsuji Nishimura[4] and Akio Ogata[1]

[1]Departments of Environmental Health and Toxicology and [2]Departments of Pharmaceutical Sciences, Tokyo Metropolitan Institute of Public Health, 3-24-1 Hyakunin-cho, Shinjuku-ku, Tokyo 169-0073, Japan
[3]Divisions of Risk Assessment and [4]Divisions of Environmental Chemistry, National Institute of Health Science, 1-18-1 Kamiyoga, Setagaya-ku, Tokyo 158-8501, Japan

(Received October 19, 2011; Accepted December 5, 2011)

ABSTRACT — Possible effects of multi-wall carbon nanotubes (MWCNTs) on immune and inflammatory responses were examined in mice. Female ICR mice were given a single intraperitoneal administration (2 mg/kg body weight) of either MWCNTs, carbon black (CB), or crocidolite (blue asbestos) and controls received a vehicle of 2% sodium carboxymethyl cellulose (CMC Na). In the peritoneal cavity of MWCNT-administered mice, the liver had changed to a rounded shape and fibrous adhesions were seen on internal organs. Peritoneal cells overexpressed mRNA for genes of T helper (Th)2 cytokines (*interleukin [IL]-4*, *IL-5*, and *IL-13*), Th17 cytokine (*IL-17*), pro-inflammatory cytokines/chemokines (*IL-1β*, *IL-33, tumor necrosis factor α,* and *monocyte chemotactic protein-1*), and *myeloid differentiation factor 88* for at least 2 weeks after the administration of MWCNTs, while those of Th1 cytokine genes (*IL-2* and *interferon γ*) were overexpressed several weeks later and expression levels remained high up to 20 weeks. In MWCNT-treated mice, the numbers of leukocytes, monocytes, and granulocytes in the peripheral blood and the expression of the leukocyte adhesion molecules, cluster of differentiation (CD)49d and CD54, on granulocytes were increased 1 week after administration and remained high up to week 20. Production of ovalbumin-specific IgM and IgG_1 was enhanced by MWCNTs. These changes were not observed after CB or crocidolite administration. Thus, this study showed that MWCNTs exhibited sustained stimulating effects on immune and inflammatory responses, unlike the other mineral fibers with structural similarities.

Key words: Multi-wall carbon nanotube, Nanomaterial, Inflammation, Immunotoxicity, Hazard characterization

INTRODUCTION

Rapid progress in nanotechnology in recent years has made it possible to produce and apply numerous new and useful nanomaterials, such as nano-TiO_2, nano-SiO_2, nano-ZnO and nano-carbon materials. These are believed to be biologically inert, although inhalation of small-sized nanomaterials can cause pulmonary inflammation and fibrosis. (Mossman and Churg, 1998; Yazdi *et al.*, 2010). Carbon forms exist in many different shapes as both elementary substances and compounds, for example, diamond, charcoal, carbon black, graphite, fullerene, and carbon nanotubes are all carbon allotropes, while graphene is a single-wall product of graphite, whose structure consists of one-atom-thick planar sheets of hexagonal-bonded carbon atoms densely packed in honeycomb crystal lattices. Carbon nanotubes are seamless cylindrical structures comprising single or multiple graphene sheets. Both single-wall carbon nanotubes (SWCNTs) and multi-wall carbon nanotubes (MWCNTs) are several micrometers in length and approximately 1-20 nanometers in diameter. These needle-like structures resemble asbestos.

It is well known that asbestos inhalation causes pulmonary inflammation and fibrosis, lung cancer, and malignant mesothelioma after relatively long latency periods (Mossman *et al.*, 1990; Hei *et al.*, 1992). However, the signaling pathways that lead to the development of these asbestos-associated diseases remain largely unknown. If

Correspondence: Atsumi Yamaguchi (E-mail: Yamaguchi@member.metro.tokyo.jp)

carbon nanotubes can create the hazards and risks similar to those associated with asbestos, they must be appropriately assessed and managed to protect human health.

In vivo effects of MWCNTs have been studied using animal models with a variety of exposure methods, such as inhalation, intratracheal instillation, pharyngeal aspiration, and intraperitoneal injection, and their effects on inflammatory responses have been described. Mice exposed to MWCNTs by inhalation caused platelet-derived growth factor (PDGF) overexpression, inflammatory cell aggregation, and recruitment of macrophages that phagocytosed MWCNTs in the lung within 1 day, followed by the subsequent development of subpleural fibrosis during weeks 2-6 (Ryman-Rasmussen *et al.*, 2009a, 2009b). Pharyngeal aspiration of MWCNTs in mice caused the rapid development of fibrosis within 7 days and a persistent granulomatous inflammation throughout a 56-day post-exposure period (Porter *et al.*, 2010). Intratracheal instillation of MWCNTs in mice caused an increase in the number of neutrophils and the levels of cytokines in bronchoalveolar lavage (BAL) fluid within 1 day, and granulomatous lesions developed and persisted until day 14 of these experiments (Park *et al.*, 2009). Intraperitoneal injection of MWCNTs given to rats (Sakamoto *et al.*, 2009) or *p53* gene heterozygously deficient mice (Takagi *et al.*, 2008) induced a long-lasting inflammation and resulted in fibrous thickening and granuloma formation in the peritoneum in association with the induction of mesothelioma.

However, despite evidences from these studies, the potential immunotoxicity of MWCNTs has not been sufficiently established till date. Thus, the present study was conducted to assess a possible involvement of MWCNTs in immune and inflammatory responses of ICR mice. Intraperitoneal administration was chosen as the exposure route for MWCNTs. Although it may not be directly relevant to humans, intraperitoneal administration in a rodent model is sensitive enough to detect weak effects of MWCNTs, which was why this strategy was adopted to identify a possible carcinogenic hazard of MWCNTs (Sakamoto *et al.*, 2009; Takagi *et al.*, 2008). In addition, intraperitoneal administration can control and ensure the relationship between administration doses and agent exposure. Furthermore, some reports have clearly indicated the detection of inhaled MWCNTs in the subpleura (Ryman-Rasmussen *et al.*, 2009a), pharyngeally-aspirated MWCNTs in the pleura (Porter *et al.*, 2010), and intraperitoneally-administered MWCNTs in the liver and mesenteric lymph nodes (Sakamoto *et al.*, 2009). These results suggest that MWCNTs are distributed to a certain extent in the entire body, regardless of the exposure route used.

MATERIALS AND METHODS

Ethical approval

Our experimental protocols were approved by the Experiments Regulation Committee and the Animal Experiment Committee of the Tokyo Metropolitan Institute of Public Health prior to beginning of these experiments and were monitored at each step of experimentation for scientific and ethical appropriateness, including concerns for animal welfare, with strict adherence to the National Institutes of Health Guidelines for the Care and Use of Laboratory Animals, Japanese Government Animal Protection and Management Law, Japanese Government Notification on Feeding and Safekeeping of Animals, and other similar laws, guidelines, and rules provided domestically and internationally.

Animals

Specific pathogen-free female Crlj:CD1(ICR) mice, 6-7 weeks old, were purchased from Charles River Japan, Inc. (Kanagawa, Japan) and acclimatized for 1 week. Mice were housed individually in plastic cages (22 × 15 × 12 cm) with cedar chip bedding and had free access to a standard diet CE2 (Nihon Clea, Inc., Tokyo, Japan) and water. The animal room was maintained at 24°C-26°C with a relative humidity of 50%-60%, with 10 ventilations per hour (drawing fresh air through a high-efficiency particulate air filter, 0.3 μm, 99.9% efficiency), and on a 12 hr light/dark cycle.

Chemicals, reagents, and kits

MWCNTs (MITSUI MWCNT-7; lot number 060125-01k) were provided by National Institute of Health Science, Tokyo, Japan. These were exactly identical to those used in carcinogenicity studies with male Fisher 344 rats (Sakamoto *et al.*, 2009) and male C57BL/6-originated mice that were heterozygously deficient in the *p53* gene (Takagi *et al.*, 2008); these reports describe their physicochemical properties. Carbon black (CB; 22 nm in diameter) was purchased from Showa Chemical Industry Co., Ltd. (Tokyo, Japan). UICC-grade crocidolite was provided by the Tokyo Metropolitan Institute of Public Health.

Ovalbumin (OVA) and bovine serum albumin (BSA) were purchased from Sigma-Aldrich Co. (St. Louis, MO, USA). Horseradish peroxidase (HRP)-conjugated anti-mouse IgM and IgG_1 antibodies were purchased from Zymed Laboratories (South San Francisco, CA, USA). 2,2'-Azino-bis(3-ethylbenzothiazoline-6-sulfonic acid) diammonium salt (ABTS) tablets, a substrate for HPR-conjugated antibodies, were purchased from Roche

Diagnostics Division (Basel, Switzerland). Monoclonal anti-OVA-IgG_1 antibody (clone OVA-14) was purchased from Sigma-Aldrich. Phycoerythrin-conjugated (PE-) anti-CD3 (derived from T cell clone 145-2C11), fluorescein isothiocyanate-conjugated (FITC-) anti-CD45R (B220) (derived from B cell clone RA3-6B2), PE- anti-CD8 (clone 53-6.7), and FITC- anti-CD4 (clone GK1.5) were purchased from Beckman Coulter, Inc. (Fullerton, CA, USA). PE-Cy5.5--anti-CD3 (clone 145-2C11), PE-Cy5.5--anti-CD45 (derived from leukocyte clone 30-F11), PE--anti-CD14 (derived from monocyte clone: Sa2-8), PE--anti-Ly-6G (derived from granulocyte clone RB6-8C5), FITC--anti-CD54 (intercellular adhesion molecule [ICAM]-1; clone YN1/1.7.4), FITC--anti-CD49d (integrin α4; clone R1-2), FITC-anti-CD11b (integrin αM; clone 1/70), and anti-CD16/CD32 (Fcγ receptor III/II; clone 93) antibodies were purchased from eBioscience, Inc. (San Diego, CA, USA). RNAprotect Cell Reagent, RNeasy Mini kit, High Capacity RNA-to-cDNA kit, TaqMan Gene Expression Master Mix, and TaqMan Gene Expression Assays Inventoried were purchased from Life Technologies Co. (Carlsbad, CA, USA).

Animal experiments

Three independent animal experiments were conducted; protocols for handling test chemicals were identical in each. MWCNTs, CB, or crocidolite was suspended in 2% sodium carboxymethyl cellulose (CMC Na) to a concentration of 0.2 mg/ml. A single intraperitoneal dose (2 mg/kg body weight) of each of these was administered to mice. In a vehicle control group, CMC Na was administered with a single intraperitoneal volume of 10 ml/kg body weight.

The first animal experiment included histopathological examination and real-time polymerase chain reaction (PCR) assays for mRNA expression of cytokine/chemokine genes. Within 32 weeks, 2 of 6 mice that were administered MWCNT died; hence, the last experiment was conducted at the end of 34 weeks after administration. Mice were maintained up to 34 weeks after their exposure to test chemicals or vehicle. From each treatment or vehicle group, 3-6 animals were chosen for assays at the end of 2, 4, 10, 20, and 34 weeks. Under light ether anesthesia, cells were collected from the abdominal cavity and suspended in 5 ml of phosphate-buffered saline (PBS), centrifuged at 1,200 rpm for 10 min, and stored in RNAprotect Cell Reagent until RNA extraction for the real-time PCR assay. Tissues and organs were harvested for histopathological examinations. Samples were fixed in neutrally buffered formalin, embedded in paraffin, and stained with sirius red for collagen or hematoxylin-eosin.

The second animal experiment included flow cytometry analysis of the peripheral blood cells. Mice were maintained up to 20 weeks after their exposure to test chemicals or vehicle. From each treatment or vehicle group, 4 animals were chosen for the assays on day 2 and at the end of 1, 2, 4, and 20 weeks. Under light ether anesthesia, approximately 1 ml of blood was collected through cardiac puncture into a syringe with 20 μl of an anticoagulant, ethylenediaminetetraacetic acid, and used for flow cytometry.

The third animal experiment included determinations of OVA-specific immunoglobulins. After their exposure to test chemicals or vehicle, mice were immunized with OVA/alum intraperitoneally administered at a dose of 100 μg/mouse on days 2 and 10 as previously described (Ito *et al.*, 2002). Under light ether anesthesia, blood samples of approximately 0.1 ml were collected from a tail vein. Samples were taken from 10 to19 animals from each treatment or vehicle group from the tail vein 8 days after the last immunization for IgM and from 15 animals from each group 20 days after the last immunization for IgG_1. Serum was stored at -80°C until assayed.

Real-time PCR assays for mRNA expression of cytokine/chemokine gene

Total RNA was isolated from 5 x 10^4 peritoneal cells obtained in the first animal experiment as described above, using RNeasy Mini kit. RNA from untreated 8-16-week-old female ICR mice were prepared separately, pooled, and used as a basal expression control. First-strand cDNA was prepared from 0.9 μg of RNA using a High Capacity RNA-to-cDNA kit. PCR used TaqMan Gene Expression Master Mix for genes (*IL-1β*, Mm01336189_m1; *IL-2*, Mm00434256_m1; *IL-4*, Mm99999154_m1; *IL-5*, Mm99999063_m1; *IL-6*, Mm99999064_m1; *IL-8*, Mm00436450_m1; *IL-10*, Mm99999062_m1; *IL-13*, Mm00434204_m1; *IL-17*, Mm00439619_m1; *IL-18*, Mm00434225_m1; *IL-33*, Mm00505403_m1; *IFNγ*, Mm99999071_m1; *MCP-1*, Mm00441242_m1; *MyD88*, Mm00440338_m1; *TGFβ1*, Mm03024053_m1; *TNFα*, Mm99999068_m1; *TATA box binding protein [TBP]*, Mm00446973_m1; *hypoxanthine phosphoribosyltransferase [HPRT]*, Mm00446968_m1), cDNA-specific TaqMan Gene Expression Assays, and an ABI 7500 Real-Time PCR System (Life Technologies). All PCR reactions were performed in duplicates. The quantity of PCR product was determined by the Comparative Ct Method as described by the manufacturer, in which each sample was normalized against the value of a housekeeping gene, *HPRT*. Fold-changes were expressed as either an increase or decrease compared with the basal expression control level.

Flow cytometry analysis of the peripheral blood cells

After 15 minute pre-incubation with an anti-CD16/32 monoclonal antibody to prevent non-specific binding, a peripheral blood sample (100 μl) obtained in the second animal experiment described above was reacted with various combinations of antibodies. After a 30-min incubation in the dark, erythrocytes were lysed with 4 ml of Tris (1 g/500 ml)plus NH_4Cl (2.8 g /500 ml) for 10 min, suspended in 4 ml of PBS, and centrifuged at 1,200 rpm for 10 min. The cell pellet was washed in PBS with 0.5% BSA. Fluorescence intensity and cell numbers were determined using a Cell Lab Quanta SC (Beckman Coulter). The number of leucocytes was counted as positive cells of PE-Cy5.5- anti-CD45 antibody. The number of lymphocytes was distinguished based on CD45 fluorescence and side scatter. T and B cells were distinguished based on PE and FITC fluorescence from PE-Cy5.5- CD45 positive cells. CD4 and CD8 cells were distinguished based on PE and FITC fluorescence from PE-Cy5.5- CD3 positive cells. Percent of CD11b, CD49d, and CD54 positive cells was measured based on FITC fluorescence from CD45 and CD14 or CD45 and Ly6G positive cells.

Serum OVA-specific immunoglobulin concentrations

Concentrations of OVA-specific IgM and IgG_1 in serum were determined using ELISA. We added 100 μl of 100 μg/ml of OVA to wells of a microtest plate and incubated the plates overnight at 4°C. Wells were washed 6 times with 0.05% Tween20/PBS (0.05T/PBS) and blocked with 5% BSA in PBS (5B/PBS) for 2 hr at room temperature. Diluted serum (IgM: 1/150, IgG_1: 1/5 x 10^6) was then added to each well and incubated for 2 hr. After 6 washes with 0.05T/PBS, the wells were blocked with 5B/PBS for 1 hr at room temperature. HRP-labeled anti-mouse IgM and IgG_1 antibodies were added to each well, and the plates were incubated for 2 hr at room temperature. After 6 washes with 0.05T/PBS, a substrate solution prepared using ABTS Tablets according to the manufacturer's instructions was added and the color reaction was allowed to develop in the dark at room temperature for 30 min. Optical density (OD) at 405 against 492 nm was determined using a microplate reader (SUNRISE REMOTE; Wako Pure Chemical Industries, Ltd., Osaka, Japan). Values for anti-OVA antibody were used as basal expression control.

Statistical analysis

Intergroup comparisons were made using Student's *t*-test. Significance level was set at p value < 0.05 .

RESULTS

General findings

During the course of the experiments, the body weights of mice increased within the same range after intraperitoneal administration of CMC Na, MWCNTs, CB, or crocidolite. In the first animal experiment, morphological assessments were conducted for mice that were given a single intraperitoneal administration of MWCNT, CB, or crocidolite. In the abdominal cavities of MWCNT-treated mice as compared with CMC Na-treated mice, liver edges had lost their sharpness, fibrous adhesions were seen on internal organs, and deposits were observed on the surfaces of the liver and diaphragm (Figs. 1a and 1b). In CB-treated mice, deposits were scattered in the abdominal cavity, especially on intestinal surfaces (Fig. 1c). No noteworthy changes were observed in the abdominal cavities of the CMC Na- or crocidolite-treated mice (Figs. 1a and 1d), or anywhere outside of the abdominal cavity in any of the groups.

Peritoneal cells obtained from MWCNT-treated mice contained small amounts of erythrocytes as compared with CMC Na-treated mice (Figs. 2a and 2b), whereas numerous erythrocytes were found for the crocidolite-treated mice (Fig. 2d). The peritoneal cells obtained from the CB-treated mice looked black, presumably because of the engulfment of the test chemical (Fig. 2c).

Fig. 3 showed the micrograms of liver, and Fig. 3a and 3b were the liver of CMC Na treated-mice that had thin layered mesothelium. Histopathological examinations revealed that the hepatic visceral peritoneum had fibrous thickening along with mesothelial cell hypertrophy in the MWCNT-treated mice (Figs. 3c and 3d). Inflammatory cells had infiltrated into this fibrously thickened visceral peritoneum. The majority of these infiltrating cells were macrophages containing MWCNTs, along with eosinophils, plasma cells, and immature myeloid cells (Fig. 3e) that occasionally formed a granulation (Fig. 3c). These changes were not observed in the CB- or crocidolite-treated mice.

No tumorigenic changes were observed either macroscopically or histopathologically in any of the mice treated with any of the test chemicals within the 34-week experimental period.

Expression of cytokine mRNA in peritoneal cells

mRNA expression levels of certain cytokine genes were substantially increased in the peritoneal cells obtained from MWCNT-treated mice, and these high levels were maintained up to the ends of 20 and 34 weeks. Th2 cytokine gene mRNA levels for *IL-4*, *IL-5*, and *IL-13*

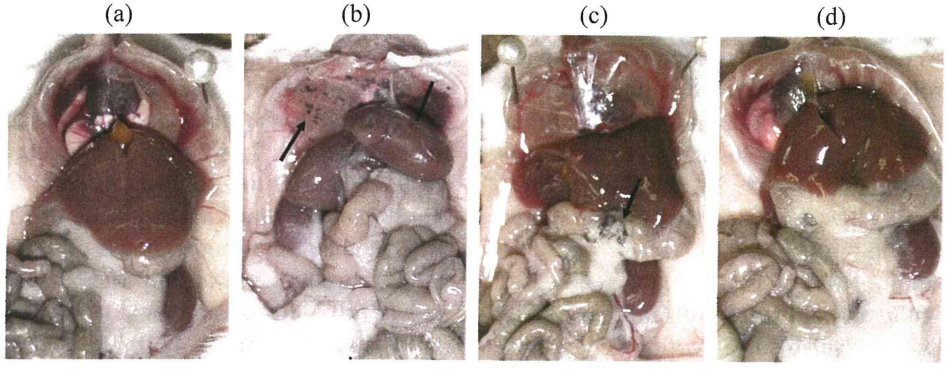

Fig. 1. Representative macroscopic appearances of the mouse abdominal cavity in the first animal experiment. Observations were made at 10 weeks after exposure to (a) CMC Na, (b) MWCNTs, (c) CB, or (d) crocidolite. Arrows indicate deposits of test chemicals.

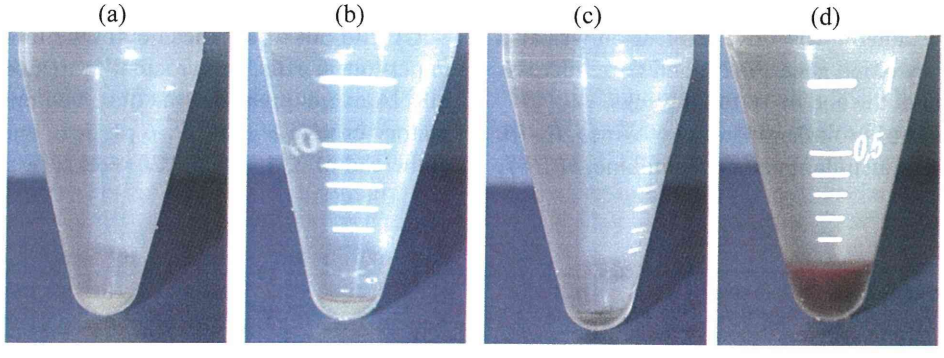

Fig. 2. Representative macroscopic appearances of peritoneal cells obtained from mice in the first animal experiment. Observations were made at 10 weeks after exposure to (a) CMC Na, (b) MWCNTs, (c) CB, or (d) crocidolite.

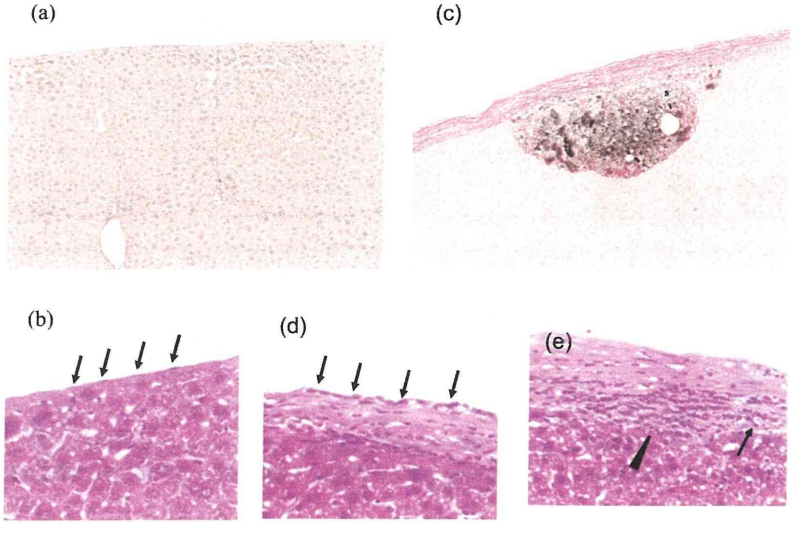

Fig. 3. Representative histology of the mouse liver in the first animal experiment. Examinations were made at 20 weeks after exposure to (a, b) CMC Na or (c-e) MWCNTs. Arrows indicate mesothelial cells and arrowheads indicate the infiltrations of eosinophils and immature myeloid cells. (a) and (c) were stained with sirius red staining, x 100, and (b), (d), and (e) were stained with hematoxylin-eosin, x 400.

were significantly increased from 2 to 20 weeks after administering MWCNTs. When compared with the basal expression control value for untreated animals, mRNA levels of *IL-4* were 34, 43, 24, 60, and 3 times higher, those of *IL-5* were 110, 127, 63, 226, and 69 times higher, and those of *IL-13* were 55, 38, 11, 28, and 3 times higher at 2, 4, 10, 20, and 34 weeks, respectively, after administering MWCNTs (Fig. 4).

Overexpression of mRNA of Th1 cytokine genes, *IL-2* and *IFNγ*, were delayed compared with mRNA of Th2 cytokine genes, but were also sustained; however, these were not significantly higher than basal expression levels except for *IL-2* at the end of 34 weeks. mRNA expression levels of *IL-2* were 0.3, 0.6, 1.5, 5.4, and 4.8 times higher, and those of *IFNγ* were 0.5, 0.3, 0.6, 1.6, and 4.3 times higher at the end of 2, 4, 10, 20, and 34 weeks, respectively (Fig. 4). Sustained mRNA overexpression was also found for a Th17 cytokine gene, *IL-17*, and these increases were significant at the end of 10 to 20 weeks.

mRNA for genes of proinflammatory cytokines, *IL-1β*, *IL-33*, and *TNFα*, and an inflammatory chemokine, *MCP-1*, were increased significantly at the end of 2 to 20 weeks (*IL-1β* and *TNFα*) and at 2 to 34 weeks (*IL-33* and *MCP-1*). mRNA level of an adapter protein of Toll-like receptors (TLR), *MyD88*, was also increased significantly at the end of week 2 to 20. mRNA levels of *IL-17* were 9, 13, 9, 26, and 25 times higher, those of *IL-1β* were 29, 23, 32, 28, and 19 times higher, those of *IL-33* were 13, 20, 5, 13, and 20 times higher, those of *TNFα* were 3, 2, 2, 3, and 2 times higher, those of *MCP-1* were 17, 28, 41, 49, and 42 times higher, and those of *MyD88* were 3, 3, 2, 2, and 1 time higher at 2, 4, 10, 20, and 34 weeks, respectively, after MWCNT administration (Figs. 4 and 5). mRNA levels of other inflammatory cytokine genes (*IL-6*, *IL-8*, and *IL-18*), anti-inflammatory cytokines (*IL-10* and *TGFβ*), and a housekeeping gene (*TBP*) were not affected by exposure to MWCNTs (Figs. 4 and 5).

CB did not affect these cytokine mRNA expressions in peritoneal cells. For crocidolite-treated mice, sustained mRNA overexpression was observed only for an inflammatory cytokine gene, *IL-6* (4, 5, 6, and 8 times higher at the end of 2, 4, 10, and 20 weeks, respectively), which

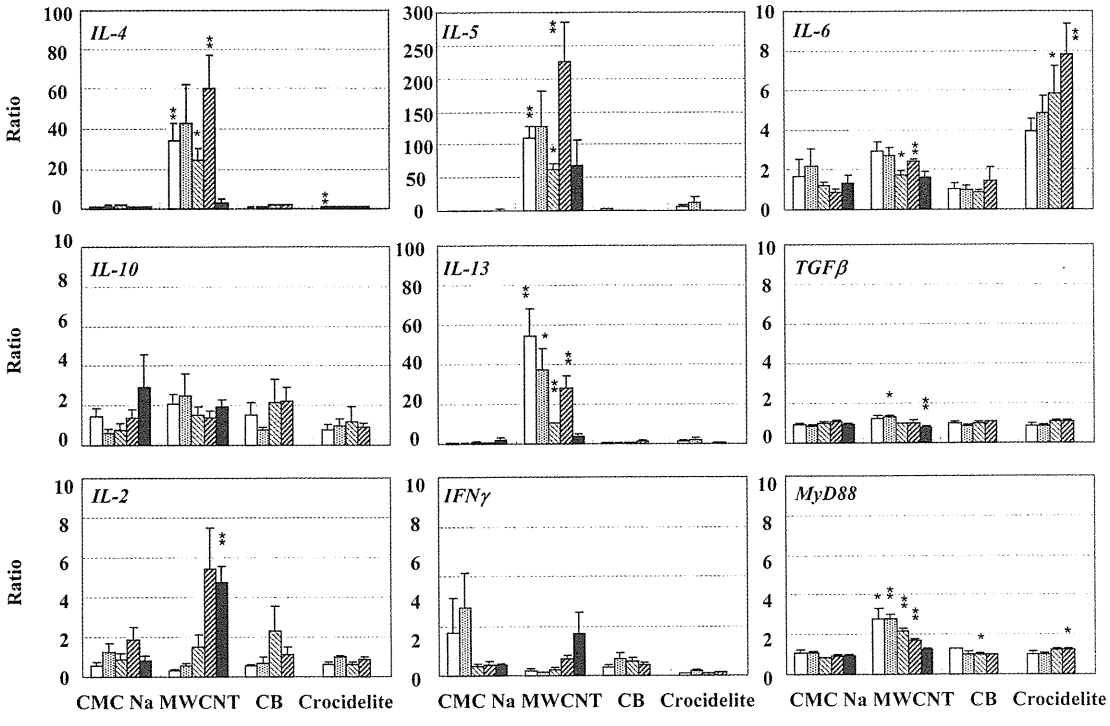

Fig. 4. mRNA expression of Th2 cytokine genes (*IL-4*, *IL-5*, *IL-10*, *IL-13*, and *TGFβ*), Th1 cytokine genes (*IL-2* and *IFNγ*), and a TLR adaptor protein (*MyD88*) in peritoneal cells obtained from mice in the first animal experiment. For each group of mice exposed to a test chemical or vehicle, columns from the left to the right are average values (n = 3-6) at 2, 4, 10, 20, and 34 weeks after exposure. These determinations were not made at the end of week 34 for the CB- and crocidolite-treated groups. (*$p < 0.05$, **$p < 0.01$).

was a more pronounced change than that with MWCNTs (Fig. 4). In addition, mRNA levels of *IL-5* were 5, 11, 1, and 1 times higher (Fig. 4), and those of *MCP-1* were 14, 9, 2, and 4 times higher (Fig. 5) at the end of 2, 4, 10, and 20 weeks, respectively; however, these changes were faint and transient.

Effects on the peripheral blood cells

MWCNT treatment increased the total number of leukocytes, granulocytes, and monocytes in the peripheral blood as early as 1 week after its administration, and these high levels were maintained up to the end of week 20 (Figs. 6a, 6b and 6c). The number of total lymphocytes was also increased, but only at the end of week 20. B and T cells were increased, although not significantly, within the 20-week experimental period in the MWCNT-treated mice (Figs. 6d, 6e and 6f). In the crocidolite treatment mice, the numbers of leukocytes, granulocytes, and monocytes exhibited a statistically significant, although minimal, transient increase at the end of week 1 (Figs. 6a, 6b and 6c). CB and crocidolite treatment increased the numbers of lymphocytes, B, and T cells at the end of day 2 and 1 week, but not significantly, and then decreased (Figs. 6d, 6e and 6f).

Expression of leukocyte adhesion molecules on the peripheral blood cells

MWCNT treatment induced overexpression of CD49d and CD54, but not CD11b, on granulocytes as early as 2 and 1 weeks, respectively, after its administration, and these high levels were maintained up to the end of week 20 (Fig. 7a). The expression of adhesion molecules was not altered on monocytes, with the exception that a statistically significant, although minimal, transient overexpression was observed for CD49d at the end of week 4 (Fig. 7b). CB and crocidolite did not induce overexpression of any of the leukocyte adhesion molecules on the peripheral blood cells, and in fact their expression was transiently decreased in some cases (Fig. 7).

OVA-specific immunoglobulins in serum

Figure 8 summarizes the results for the serum con-

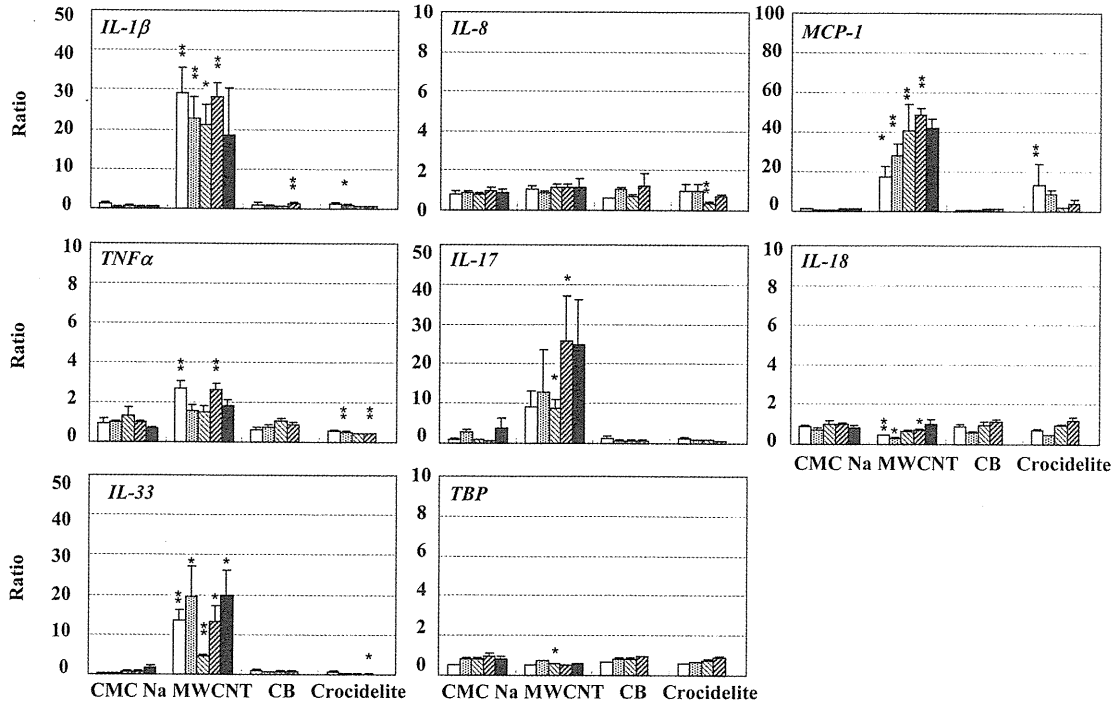

Fig. 5. mRNA expression of inflammatory cytokine genes in peritoneal cells obtained from mice in the first animal experiment. For each group of mice exposed to a test chemical or vehicle, columns from the left to the right are average values (n = 3-6) at 2, 4, 10, 20, and 34 weeks after exposure. These determinations were not made at the end of week 34 for the CB- and crocidolite-treated groups. (*$p < 0.05$, **$p < 0.01$).

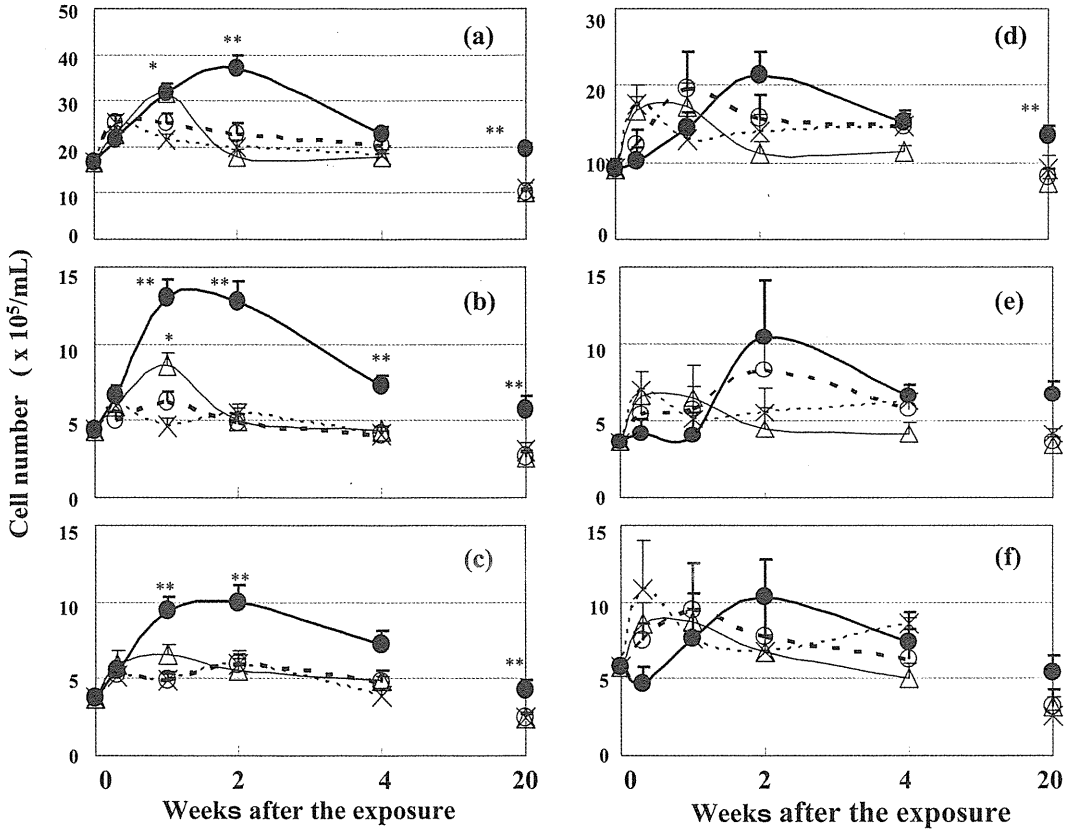

Fig. 6. Flow cytometry results for the peripheral blood cells obtained from mice in the second animal experiment. Changes in the numbers of (a) leukocytes, (b) granulocytes, (c) monocytes, (d) lymphocytes, (e) B cells, and (f) T cells after exposure to CMC Na (open circles), MWCNTs (closed circles), CB (crosses), and crocidolite (open triangles). Results are means ± standard deviations (n = 4). Asterisks indicate that results are significantly different from those of controls (*$p < 0.05$, **$p < 0.01$).

centrations of OVA-specific IgM (Fig. 8a) and IgG_1 (Fig. 8b). For mice treated with MWCNTs, CB, crocidolite, and CMC Na, the relative amounts (arbitrary units; AU) of OVA-specific IgM were, 1.33 ± 0.20, 1.07 ± 0.20, 1.07 ± 0.15, and 0.79 ± 0.12 AU, respectively, while those for OVA-specific IgG_1 were, 3.68 ± 0.57, 2.49 ± 0.29, 2.13 ± 0.32, and 2.28 ± 0.35 AU, respectively. Thus, MWCNT and not CB or crocidolite, significantly enhanced the production of OVA-specific immunoglobulins in mice.

DISCUSSION

The present study clearly shows that MWCNTs stimulated immune and inflammatory responses in mice and these effects sustained until the mice died. It has been previously shown in other animal models that a single intraperitoneal administration of MWCNT caused severe inflammation throughout the abdominal cavity and mesothelioma. Male Fisher 344 rats died at 37-52 weeks after administration (Sakamoto *et al.*, 2009) and and male C57BL/6-originated mice heterozygously deficient in the *p53* gene died within 25 weeks of administration (Takagi *et al.*, 2008).

The toxicity caused by MWCNTs in the present study did not involve tumor formation, but did induce severe inflammation, and 2 of 6 mice had died by the end of 32 weeks. The differences in the magnitudes of MWCNT toxicity between the present and previous studies was apparently because of differences in species, strains, and/or genders. To extrapolate the animal toxicity data to information important for human health concerns, further investigations are required. The most aggressive morphological change we observed was the infiltration of macrophages, eosinophils, plasma cells, and immature myeloid cells into the fibrously thickened visceral peritoneum of the liver with occasional granulation, and severe fibrous adhesions to the internal organs.

Light microscopic examination revealed that MWCNT

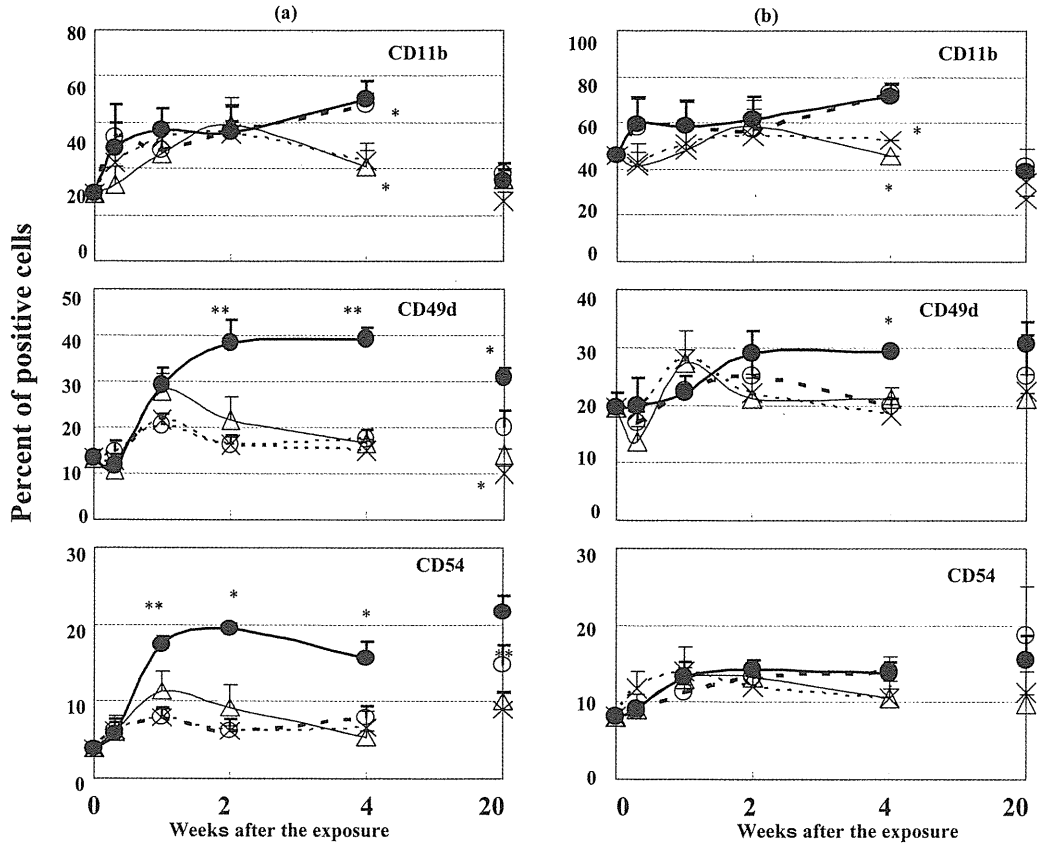

Fig. 7. Flow cytometry results for the peripheral blood cells obtained from mice in the second animal experiment. Changes in the expression of adhesion molecules on the surfaces of (a) granulocytes and (b) monocytes after exposure to CMC Na (open circles), MWCNT (closed circles), CB (crosses), and crocidolite (open triangles). Results are means ± S.D. (n = 4). Asterisks indicate that values are significantly different from those of controls ($*p < 0.05$).

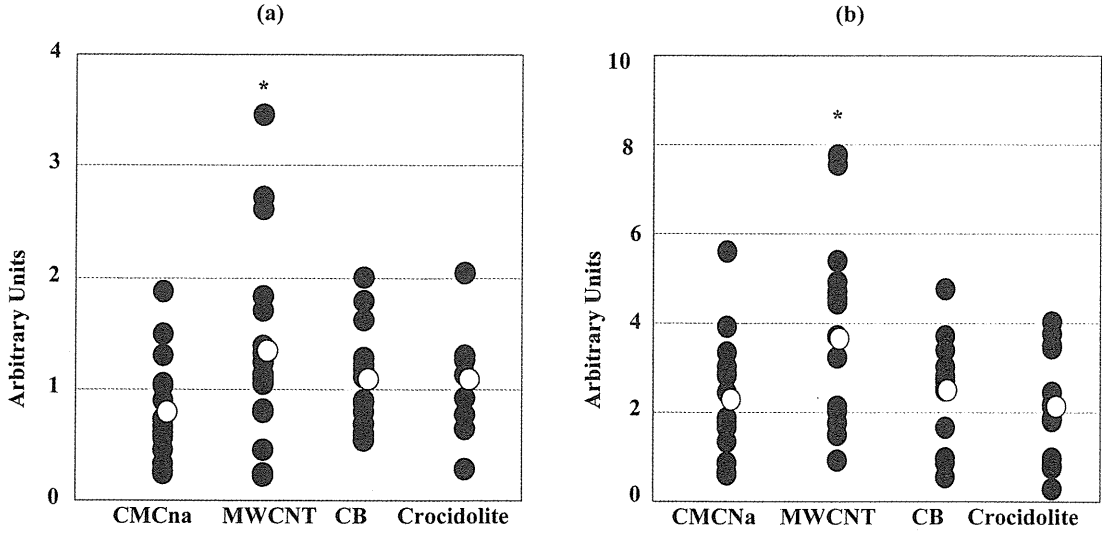

Fig. 8. Production of OVA-specific antibodies by mice in the third animal experiment. Serum concentrations of OVA-specific (a) IgM and (b) IgG_1 Open circles are average values, and closed circles are individual values (n = 10-19 for IgM, and n = 15 for IgG_1). Asterisks indicate that values are significantly different from those of controls ($*p < 0.05$).

were present in macrophages in these lesions. Frustrated phagocytosis has frequently been postulated to be involved in the mechanisms by which MWCNTs causes toxicity, including inflammation and carcinogenesis (Poland *et al.*, 2008). Thus, these lesions may have some fundamental biological importance. The sustained overexpression of cytokine mRNA in peritoneal cells may suggest one possibility, although no MWCNTs were observed in the peritoneal cells by light microscopy. An *in vitro* time lapse experiment revealed that dead cells with MWCNTs had been re-engulfed by other macrophages (data not shown), suggesting a cycle of sustained inflammation. MWCNTs either could not be limited by granuloma formation or subvisible MWCNTs may remain in the cavity. Thus, macrophages may continue their phagocytic activity, and as a result inflammatory cytokines/chemokines would be continuously produced.

Our results indicated that MWCNTs caused a systemic inflammation that was sustained for at least 20-34 weeks after a single intraperitoneal administration, because the numbers of leukocytes, granulocytes, and monocytes in the peripheral blood were increased from 1 to 20 weeks after MWCNT administration. During a similar period, CD49d and CD54 were overexpressed on granulocytes, which may have been involved in their infiltration into the inflammatory sites past vascular endothelial cells. Crocidolite increased the numbers of leukocytes, granulocytes, and monocytes at 1 week, but returned to the basal level after 2 weeks, and the effects were weaker than MWCNTs. The number of leukocytes was slightly increased at 2 days and 1 week after CMCNa exposure, and mRNA level of *IFNγ* was increased at 2 and 4 weeks after CMCNa exposure, but decreased thereafter. However the effect of CMCNa has not been known, there is a possibility CMCNa acts as a xenobiotic although the effect is little. Furthermore, the number of peripheral lymphocytes was also increased at 20 weeks after MWCNT administration, and this corresponded to the enhanced T cell-dependent production of OVA-specific antibodies, as indicated by their increased serum concentrations. The overexpressed mRNA of Th2 cytokine genes seen in peritoneal cells suggested that these cytokines have been involved in this enhanced antibody production. Although the underlying mechanisms need to be clarified, MWCNTs may promote these immune responses by acting as an adjuvant (Inoue *et al.*, 2009; Nygaard *et al.*, 2009).

The present study demonstrated the overexpression of mRNA for various cytokines/chemokines in peritoneal cells after a single intraperitoneal administration of MWCNTs. To the best of our knowledge, this is the first report of results obtained for peritoneal cells with regard to changes in cytokine/chemokine mRNA expression after MWCNT exposure *in vivo*. Previous reports focused primarily on short-term effects of MWCNT exposure. Mitchell *et al.* (2007) reported that *IL-10* levels increased in spleen homogenates after 14 consecutive days of whole body inhalation exposure for male C54BL/6 mice. Park *et al.* (2009) found that the protein levels of proinflammatory cytokines were increased both in the BAL fluid and in the peripheral blood, in which Th2 cytokines were increased to a greater extent than Th1 cytokines, in mice given intratracheal administrations of MWCNTs. In these reports, the levels of cytokines reached a peak at day 1 after the exposure and remained high at day 14.

In a study by Ryman-Rasmussen *et al.* (2009b) intratracheally administered MWCNTs potentiated the development of airway fibrosis in mice with allergic asthma induced by OVA sensitization, in which the levels of *IL-13* and *IL-5* increased at day 1, but returned to normal levels at day 14 when airway fibrosis became significant. Inoue *et al.* (2009) used MWCNT instillation for 6 weeks. At 24 hours after the final treatment, they observed significant exacerbation of murine allergic airway inflammation and high levels of Th1 and Th2 cytokine proteins. In the present study, the time-courses of changes in mRNA levels corresponded to functional groups of cytokines/chemokines.

mRNA overexpression of some pro-inflammatory cytokine genes, *IL-1β and IL-33*, occurred within 2 weeks and remained elevated up to the end of week 34. These are known to induce Th2 cytokines (Schmitz *et al.*, 2005; Amatucci *et al.*, 2007; Komai-Koma *et al.*, 2007; Kondo *et al.*, 2008). Therefore, mRNA of Th2 cytokine genes, *IL-4*, *IL-5* and *IL-13*, were also overexpressed within 2 weeks and remained elevated up to week 20. Among these, mRNA level for *IL-5* was still high, but levels for *IL-4* and *IL-13* decreased at the end of week 34.

mRNA level of a Th17 cytokine gene, *IL-17*, was also increased within 2 weeks, it was increased significantly after 10 to 20 weeks, and was still high, although not significantly, at the end of week 34. mRNA of Th1 cytokine genes, *IL-2* and *IFNγ*, were also overexpressed; however, this occurred at 20-34 weeks (*IL2*) and 34 weeks (*IFNγ*) after MWCNT exposure. While the details of the underlying mechanisms need to be clarified, the differential, time-dependent overexpression of Th2 and Th17 cytokine genes at first followed by Th1 cytokine genes may provide for some optimum balance between these inflammatory mediators for the sustained stimulating effects of MWCNTs on immune and inflammatory responses.

The present study indicated a rapid, drastic and sus-

tained increase in mRNA levels of Th2 cytokine genes, *IL-4*, *IL-5*, and *IL-13*, in peritoneal cells after exposure to MWCNT. In asthmatic and atopic patients, Th2 cytokines are induced and enhance inflammation and fibrosis (Schmid-Grendelmeier *et al.*, 2002; Izuhara 2003; Doherty and Broide 2007; Choi *et al.*, 2008). Thus, the overexpression of the Th2 cytokine genes in the present study may indicate their critical roles in MWCNT-induced inflammatory changes.

Among these overexpressed Th2 cytokines, mRNA level of *IL-5* increased most strikingly; it was 100 times higher than the control level at the end of week 2 and 50 times higher even at the end of week 34. Administration of an anti-*IL-5* antibody to mild atopic asthmatic patients reduced the numbers of airway eosinophils and fibrosis (Flood-Page *et al.*, 2003), and that *IL-5* deficient mice have significantly less peribronchial fibrosis (total collagen content) and significantly less peribronchial smooth muscle (thickness of peribronchial smooth muscle layer, α-smooth muscle actin immunostaining; Cho *et al.*, 2004). Thus, *IL-5* may be biologically important in the inflammatory reactions related to immune system disturbances. In these reports, *IL-5* and *TGFβ* were involved in the infiltration of eosinophils. Although the mRNA level of *TGFβ* was not altered in the present study, *IL-5* overexpresion may have caused the eosinophil infiltration into inflammatory sites.

It has recently been shown that *IL-1β, IL-18*, and *IL-33* are produced by the innate immune system, followed by the subsequent induction of Th2 cytokines (Schmid-Grendelmeier *et al.*, 2002; Izuhara, 2003; Doherty and Broide, 2007; Choi, *et al.*, 2008; Kroeger, *et al.*, 2009). Microbial pathogens, dead cells, and foreign bodies, such as asbestos or silica, can impose stress on phagocytes, which then develop inflammasomes.

The inflammasome is a multi-protein complex that is activated by ligand-induced intermediates, such as reactive oxygen species (ROS), K^+ efflux, or by lysosome destabilization (Dostert *et al.*, 2008; Petrilli *et al.*, 2007; Hornung *et al.*, 2008), and then by cysteine protease caspase-1. (Martinon *et al.*, 2002). Caspase-1 can initiate an apoptotic pathway and, at the same time, cleave cytokine precursors, such as pro-*IL-1β* and pro-*IL-18*, to form their mature forms (Dostert *et al.*, 2008; Yazdi *et al.*, 2010).

IL-33 is another member of the *IL-1* family that is produced by endothelial cells, epithelial cells (Moussion *et al.*, 2008), and myeloid cells (Schmitz *et al.*, 2005; Nile *et al.*, 2010). *IL-33* is processed by caspases in a manner similar to *IL-1β* and *IL-18* during apoptosis, although its cleavage product is not biologically active, and the full active form of *IL-33* must be released from damaged or necrotic cells. *IL-1β, IL-18*, and *IL-33* have been shown to activate Th2 cells, eosinophils, basophils, and mast cells to produce Th2 cytokines (Chow *et al.*, 2010; Komai-Koma *et al.*, 2007; Kondo *et al.*, 2008; Schmitz *et al.*, 2005), which induce inflammatory, allergic, and fibrotic changes (Finkelman *et al.*, 1999; Choi *et al.*, 2008; Doherty and Broide 2007).

In the present study, the mRNAs of *IL-1β* and *IL-33*, but not *IL-18*, were shown to be overexpressed, which suggests the involvement of the innate immune system in MWCNT-induced inflammatory changes. This may also be supported by the observation of the mRNA overexpression of the TLR adapter protein gene *MyD88*. TLR-related signals can also activate caspase-1 and may be a minor pathway in MWCNT-induced innate immune responses, because the magnitude of the overexpression of *MyD88* was small, although significantly increased.

The present results indicate that MWCNTs exert stronger effects than CB or crocidolite in female ICR mice. The latter two did not cause any particular pathological changes, and there were no apparent increases in leukocyte numbers, increased expression of leukocyte adhesion molecules on the peripheral blood cells, or enhanced production of OVA-specific antibodies. In addition, CB did not induce overexpression of any cytokine mRNAs in peritoneal cells, even though phagocytic activity may have been involved for up to 20 weeks. In fact, previous reports described no adverse effects of CB (Tabet *et al.*,2009; Teeguarden *et al.*, 2011). Crocidolite caused a sustained overexpression of *IL-6* mRNA in peritoneal cells, but *IL-6* has been reported not to stimulate or injure vascular vessel permeability (Manhiani *et al.*, 2007; McClintock *et al.*, 2005).

In conclusion, under the present experimental conditions, MWCNTs exhibited sustained stimulating effects on immune and inflammatory responses, unlike the other mineral fibers with structural similarities.

ACKNOWLEDGMENTS

The authors thank Messrs. Katsuhito Yuzawa and Akimichi Nagasawa for their superb technical assistance. This work was supported in part by a research budget of the Tokyo Metropolitan Government, Japan, and a Grant-in-Aid from the Ministry of Health, Labour and Welfare of Japan.

REFERENCES

Amatucci, A., Novobrantseva, T., Gilbride, K., Brickelmaier, M., Hochman, P. and Ibraghimov, A. (2007): Recombinant ST2 boosts hepatic Th2 response in vivo. J. Leukoc. Biol., **82**, 124-132.

Cho, J.Y., Miller, M., Baek, K.J., Han, J.W., Nayar, J., Lee, S.Y., McElwain, K., McElwain, S., Friedman, S. and Broide, D.H. (2004): Inhibition of airway remodeling in IL-5-deficient mice. J. Clin. Invest., **113**, 551-560.

Choi, M., Cho, W.S., Han, B.S., Cho, M., Kim, S.Y., Yi, J.Y., Ahn, B., Kim, S.H. and Jeong, J. (2008): Transient pulmonary fibrogenic effect induced by intratracheal instillation of ultrafine amorphous silica in A/J mice. Toxicol. Lett., **182**, 97-101.

Chow, J.Y., Wong, C.K., Cheung, P.F. and Lam, C.W. (2010): Intracellular signaling mechanisms regulating the activation of human eosinophils by the novel Th2 cytokine IL-33: implications for allergic inflammation. Cell. Mol. Immunol., **7**, 26-34.

Doherty, T. and Broide, D. (2007): Cytokines and growth factors in airway remodeling in asthma. Curr. Opin. Immunol., **19**, 676-680.

Dostert, C., Petrilli, V., Van Bruggen, R., Steele, C., Mossman, B.T. and Tschopp, J. (2008): Innate immune activation through Nalp3 inflammasome sensing of asbestos and silica. Science, **320**, 674-677.

Finkelman, F.D., Wynn, T.A., Donaldson, D.D. and Urban, J.F. (1999): The role of IL-13 in helminth-induced inflammation and protective immunity against nematode infections. Curr. Opin. Immunol., **11**, 420-426.

Flood-Page, P., Menzies-Gow, A., Phipps, S., Ying, S., Wangoo, A., Ludwig, M.S., Barnes, N., Robinson, D. and Kay, A.B. (2003): Anti-IL-5 treatment reduces deposition of ECM proteins in the bronchial subepithelial basement membrane of mild atopic asthmatics. J. Clin. Invest., **112**, 1029-1036.

Hei, T.K., Piao, C.Q., He, Z.Y., Vannais, D. and Waldren, C.A. (1992): Chrysotile fiber is a strong mutagen in mammalian cells. Cancer Res., **52**, 6305-6309.

Hornung, V., Bauernfeind, F., Halle, A., Samstad, E.O., Kono, H., Rock, K.L., Fitzgerald, K.A. and Latz, E. (2008): Silica crystals and aluminum salts activate the NALP3 inflammasome through phagosomal destabilization. Nat. Immunol., **9**, 847-856.

Inoue, K., Koike, E., Yanagisawa, R., Hirano, S., Nishikawa, M. and Takano, H. (2009): Effects of multi-walled carbon nanotubes on a murine allergic airway inflammation model. Toxicol. Appl. Pharmacol., **237**, 306-316.

Ito, T., Inouye, K., Fujimaki, H., Tohyama, C. and Nohara, K. (2002): Mechanism of TCDD-induced suppression of antibody production: effect on T cell-derived cytokine production in the primary immune reaction of mice. Toxicol. Sci., **70**, 46-54.

Izuhara, K. (2003): The role of interleukin-4 and interleukin-13 in the non-immunologic aspects of asthma pathogenesis. Clin. Chem. Lab. Med., **41**, 860-864.

Komai-Koma, M., Xu, D., Li, Y., McKenzie, A.N., McInnes, I.B. and Liew, F.Y. (2007): IL-33 is a chemoattractant for human Th2 cells. Eur. J. Immunol., **37**, 2779-2786.

Kondo, Y., Yoshimoto, T., Yasuda, K., Futatsugi-Yumikura, S., Morimoto, M., Hayashi, N., Hoshino, T., Fujimoto, J. and Nakanishi, K. (2008): Administration of IL-33 induces airway hyperresponsiveness and goblet cell hyperplasia in the lungs in the absence of adaptive immune system. Int. Immunol., **20**, 791-800.

Kroeger, K.M., Sullivan, B.M. and Locksley, R.M. (2009): IL-18 and IL-33 elicit Th2 cytokines from basophils via a MyD88- and p38alpha-dependent pathway. J. Leukoc. Biol., **86**, 769-778.

Manhiani, M.M., Quigley, J.E., Socha, M.J., Motamed, K. and Imig, J.D. (2007): IL6 suppression provides renal protection independent of blood pressure in a murine model of salt-sensitive hypertension. Kidney Blood Press Res., **30**, 195-202.

Martinon, F., Burns, K. and Tschopp, J. (2002): The inflammasome: a molecular platform triggering activation of inflammatory caspases and processing of proIL-beta. Mol. Cell., **10**, 417-426.

McClintock, S.D., Barron, A.G., Olle, E.W., Deogracias, M.P., Warner, R.L., Opp, M and Johnson, K.J. (2005): Role of interleukin-6 in immune complex induced models of vascular injury. Inflammation, **29**, 154-162.

Mitchell, L.A., Gao, J., Wal, R.V., Gigliotti, A., Burchiel, S.W. and McDonald, J.D. (2007): Pulmonary and systemic immune response to inhaled multiwalled carbon nanotubes. Toxicol. Sci., **100**, 203-214.

Mossman, B.T., Bignon, J., Corn, M., Seaton, A. and Gee, J.B. (1990): Asbestos: scientific developments and implications for public policy. Science, **247**, 294-301.

Mossman, B.T. and Churg, A. (1998): Mechanisms in the pathogenesis of asbestosis and silicosis. Am. J. Respir. Crit. Care. Med., **157**, 1666-1680.

Moussion, C., Ortega, N. and Girard, J.P. (2008): The IL-1-like cytokine IL-33 is constitutively expressed in the nucleus of endothelial cells and epithelial cells in vivo: a novel 'alarmin'? PLoS One, **3**, e3331.

Nile, C.J., Barksby, E., Jitprasertwong, P., Preshaw, P.M. and Taylor, J.J. (2010): Expression and regulation of interleukin-33 in human monocytes. Immunology, **130**, 172-180.

Nygaard, U.C., Hansen, J.S., Samuelsen, M., Alberg, T., Marioara, C.D. and Lovik, M. (2009): Single-walled and multi-walled carbon nanotubes promote allergic immune responses in mice. Toxicol. Sci., **109**, 113-123.

Park, E.J., Cho, W.S., Jeong, J., Yi, J., Choi, K. and Park, K. (2009): Pro-inflammatory and potential allergic responses resulting from B cell activation in mice treated with multi-walled carbon nanotubes by intratracheal instillation. Toxicology, **259**, 113-121.

Petrilli, V., Papin, S., Dostert, C., Mayor, A., Martinon, F. and Tschopp, J. (2007): Activation of the NALP3 inflammasome is triggered by low intracellular potassium concentration. Cell Death Differ **14**, 1583-1589.

Poland, C.A., Duffin, R., Kinloch, I., Maynard, A., Wallace, W.A., Seaton, A., Stone, V., Brown, S., Macnee, W. and Donaldson, K. (2008): Carbon nanotubes introduced into the abdominal cavity of mice show asbestos-like pathogenicity in a pilot study. Nat. Nanotechnol., **3**, 423-428.

Porter, D.W., Hubbs, A.F., Mercer, R.R., Wu, N., Wolfarth, M.G., Sriram, K., Leonard, S., Battelli, L., Schwegler-Berry, D., Friend, S., Andrew, M., Chen, B.T., Tsuruoka, S., Endo, M. and Castranova, V. (2010): Mouse pulmonary dose- and time course-responses induced by exposure to multi-walled carbon nanotubes. Toxicology, **269**, 136-147.

Ryman-Rasmussen, J.P., Cesta, M.F., Brody, A.R., Shipley-Phillips, J.K., Everitt, J.I., Tewksbury, E.W., Moss, O.R., Wong, B.A., Dodd, D.E., Andersen, M.E. and Bonner, J.C. (2009a): Inhaled carbon nanotubes reach the subpleural tissue in mice. Nat. Nanotechnol., **4**, 747-751.

Ryman-Rasmussen, J.P., Tewksbury, E.W., Moss, O.R., Cesta, M.F., Wong, B.A. and Bonner, J.C. (2009b): Inhaled multiwalled carbon nanotubes potentiate airway fibrosis in murine allergic asthma. Am. J. Respir. Cell. Mol. Biol., **40**, 349-358.

Sakamoto, Y., Nakae, D., Fukumori, N., Tayama, K., Maekawa, A., Imai, K., Hirose, A., Nishimura, T., Ohashi, N. and Ogata, A. (2009): Induction of mesothelioma by a single intrascrotal administration of multi-wall carbon nanotube in intact male Fischer 344 rats. J. Toxicol. Sci., **34**, 65-76.

Schmid-Grendelmeier, P., Altznauer, F., Fischer, B., Bizer, C.,

Straumann, A., Menz, G., Blaser, K., Wüthrich, B. and Simon, H.U. (2002): Eosinophils express functional IL-13 in eosinophilic inflammatory diseases. J. Immunol., **169**, 1021-1027.

Schmitz, J., Owyang, A., Oldham, E., Song, Y., Murphy, E., McClanahan, T.K., Zurawski, G., Moshrefi, M., Qin, J., Li, X., Gorman, D.M., Bazan, J.F. and Kastelein, R.A. (2005): IL-33, an interleukin-1-like cytokine that signals via the IL-1 receptor-related protein ST2 and induces T helper type 2-associated cytokines. Immunity, **23**, 479-490.

Tabet, L., Bussy, C., Amara, N., Setyan, A., Grodet, A., Rossi, M.J., Pairon, J.C., Boczkowski, J. and Lanone, S. (2009): Adverse effects of industrial multiwalled carbon nanotubes on human pulmonary cells. J. Toxicol. Environ. Health A, **72**, 60-73.

Takagi, A., Hirose, A., Nishimura, T., Fukumori, N., Ogata, A., Ohashi, N., Kitajima, S. and Kanno, J. (2008): Induction of mesothelioma in p53+/- mouse by intraperitoneal application of multi-wall carbon nanotube. J. Toxicol. Sci., **33**, 105-116.

Teeguarden, J.G., Webb-Robertson, B.J., Waters, K.M., Murray, A.R., Kisin, E.R., Varnum, S.M., Jacobs, J.M., Pounds, J.G., Zanger, R.C. and Shvedova, A.A. (2011): Comparative proteomics and pulmonary toxicity of instilled single-walled carbon nanotubes, crocidolite asbestos, and ultrafine carbon black in mice. Toxicol. Sci., **120**, 123-135.

Yazdi, A.S., Guarda, G., Riteau, N., Drexler, S.K., Tardivel, A., Couillin, I. and Tschopp, J. (2010): Nanoparticles activate the NLR pyrin domain containing 3 (Nlrp3) inflammasome and cause pulmonary inflammation through release of IL-1alpha and IL-1beta. Proc. Natl. Acad. Sci. USA, **107**, 19449-19454.

Hindawi Publishing Corporation
Journal of Nanotechnology
Volume 2012, Article ID 101243, 6 pages
doi:10.1155/2012/101243

Research Article

Raman Laser Polymerization of C_{60} Nanowhiskers

Ryoei Kato and Kun'ichi Miyazawa

National Institute for Materials Science, Fullerene Engineering Group, 1-1, Namiki, Ibaraki, Tsukuba 305-0044, Japan

Correspondence should be addressed to Kun'ichi Miyazawa, miyazawa.kunichi@nims.go.jp

Received 14 July 2011; Revised 25 December 2011; Accepted 4 January 2012

Academic Editor: Junfeng Geng

Photopolymerization of C_{60} nanowhiskers (C_{60}NWs) was investigated by using a Raman spectrometer in air at room temperature, since the polymerized C_{60}NWs are expected to exhibit a high mechanical strength and a thermal stability. Short C_{60}NWs with a mean length of 4.4 μm were synthesized by LLIP method (liquid-liquid interfacial precipitation method). The $A_g(2)$ peak of C_{60}NWs shifted to the lower wavenumbers with increasing the laser beam energy dose, and an energy dose more than about 1520 J/mm^2 was found necessary to obtain the photopolymerized C_{60}NWs. However, excessive energy doses at high-power densities increased the sample temperature and lead to the thermal decomposition of polymerized C_{60} molecules.

1. Introduction

C_{60} nanowhiskers (C_{60}NWs) are the single crystal nanofibers composed of C_{60} molecules [1] and can be synthesized by a facile method called "LLIP method" [2]. C_{60}NWs have a variety of applications and such as field-effect transistors (FETs) [3], solar cells [4], biosensors [5].

C_{60} molecules can be polymerized by electron beam irradiation [6]. Although as-grown C_{60}NWs are composed of the C_{60} molecules that are weakly bonded via van der Waals forces [7], the C_{60}NWs irradiated by electron beams showed the stronger thermal stability [8], the higher Young's modulus [9] than pristine van der Waals C_{60} crystals. Hence, it is of great importance to study the polymerization of C_{60}NWs in order to improve their mechanical and thermal properties.

Laser irradiation is a promising method to obtain the polymerized C_{60} molecules [7, 10]. We first showed the photopolymerization of C_{60}NWs by using the Raman laser beam irradiation [7]. Rao et al. showed that the peak of $A_g(2)$ pentagonal pinch mode of C_{60} shifts downward from 1469 cm^{-1} to 1459 cm^{-1} upon the photopolymerization [11], showing that the shift of $A_g(2)$ peak is a good indicator for the polymerization of C_{60}.

Alvarez-Zauco et al. studied the polymerization of C_{60} thin films in air by the ultraviolet (UV) laser irradiation as a function of laser energy dose (= fluence) from 10 to 50 mJ/cm^2 in order to optimize the photopolymerization of C_{60} films [12]. Likewise, the laser energy dose for the photopolymerization of C_{60}NWs should be optimized. Hence, the present study aims to reveal how the polymerization of C_{60}NWs proceeds as a function of the laser beam energy dose.

2. Experimental

C_{60}NWs were synthesized by a modified liquid-liquid interfacial precipitation method. Isopropyl alcohol (IPA) was gently poured into a toluene solution saturated with C_{60} (MTR Ltd. 99.5%) in a glass bottle to make a liquid-liquid interface, and then the solution was subjected to ultrasonication and stored in an incubator at 10°C to grow short C_{60}NWs. The synthesized C_{60}NWs were filtered and dried in vacuum at 100°C for 120 min. to remove the solvents. In the Raman spectrometry analyses, the C_{60}NWs dispersed in ethyl alcohol were mounted on a slide glass and dried in air.

A Raman spectrometer (JASCO, NRS-3100) with a green laser of 532 nm excitation wavelength was used for the polymerization and structural analysis of C_{60}NWs in air. The power of laser light illuminated onto the specimens was measured by using a silicon photodiode (S2281, Hamamatsu Photonics K.K.). The laser beam power density (D) and

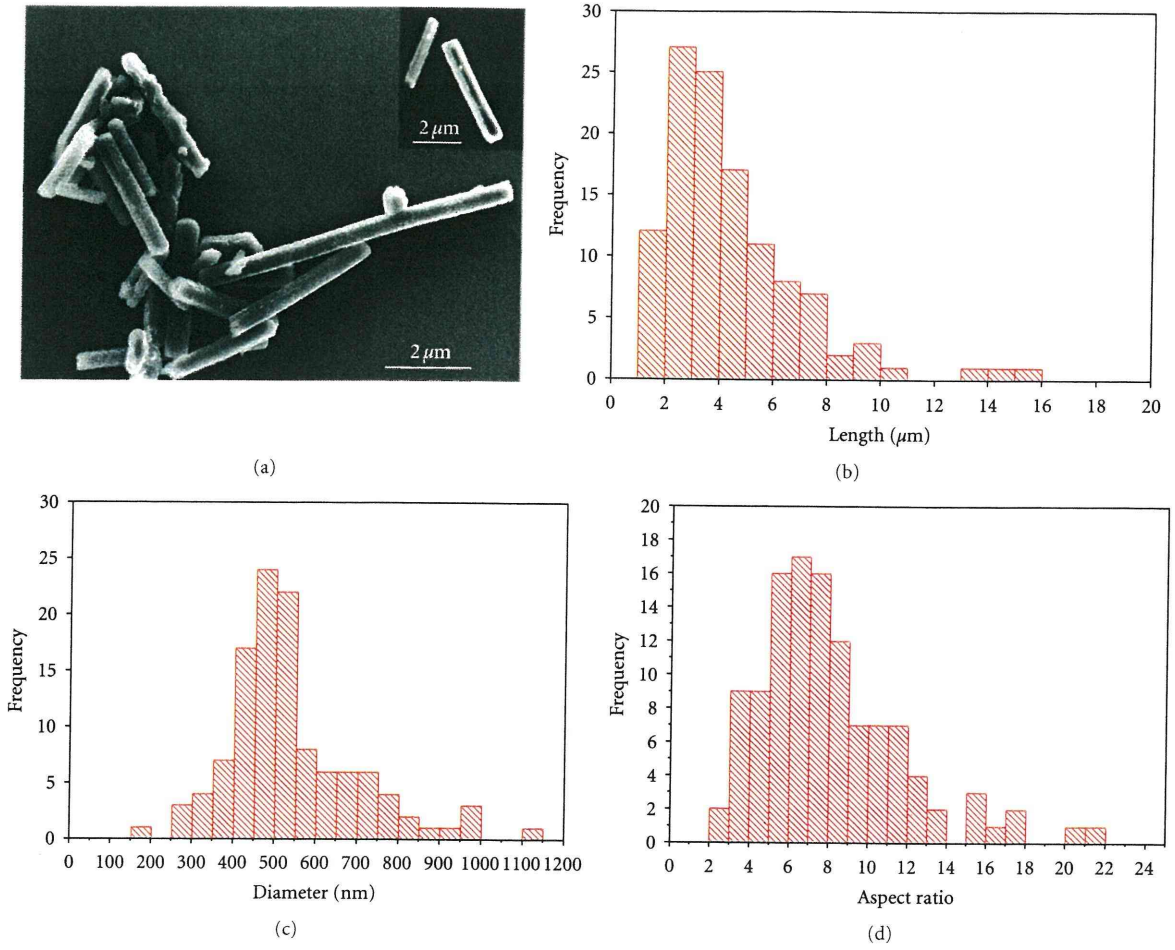

FIGURE 1: (a) SEM images, (b) length, (c) diameter, and (d) aspect ratio (length/diameter) distributions of the synthesized C_{60}NWs.

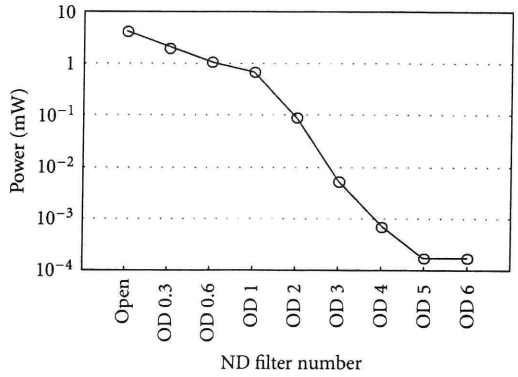

FIGURE 2: Relationship between the neutral density (ND) filter number and the laser beam power.

the energy dose of excitation laser beams in the Raman spectroscopy were controlled by changing ND (Neutral Density) filters, the defocus value of objective lens, and the exposure time of laser beam. D is defined by the following formula in this paper,

$$D\ (\mathrm{mW/mm^2}) = \frac{\text{The power of laser beam (mW)}}{\text{the area of laser beam exposed on the sample (mm}^2\text{)}}. \quad (1)$$

3. Results and Discussion

Figure 1 shows examples of scanning electron microscopy (SEM) images and the size distributions of the synthesized C_{60}NWs with a mean length of 4.4 ± 2.7 μm and a mean diameter of 540 ± 161 nm. The distribution of aspect ratios (length/diameter) is also shown. Most of the C_{60}NWs were found to possess the aspect ratios less than 15.

The power of excitation laser beam can be changed by selecting ND filters. Figure 2 shows the relationship between the ND filter number and the power of laser beam irradiated on samples. The laser beam power could be widely changed

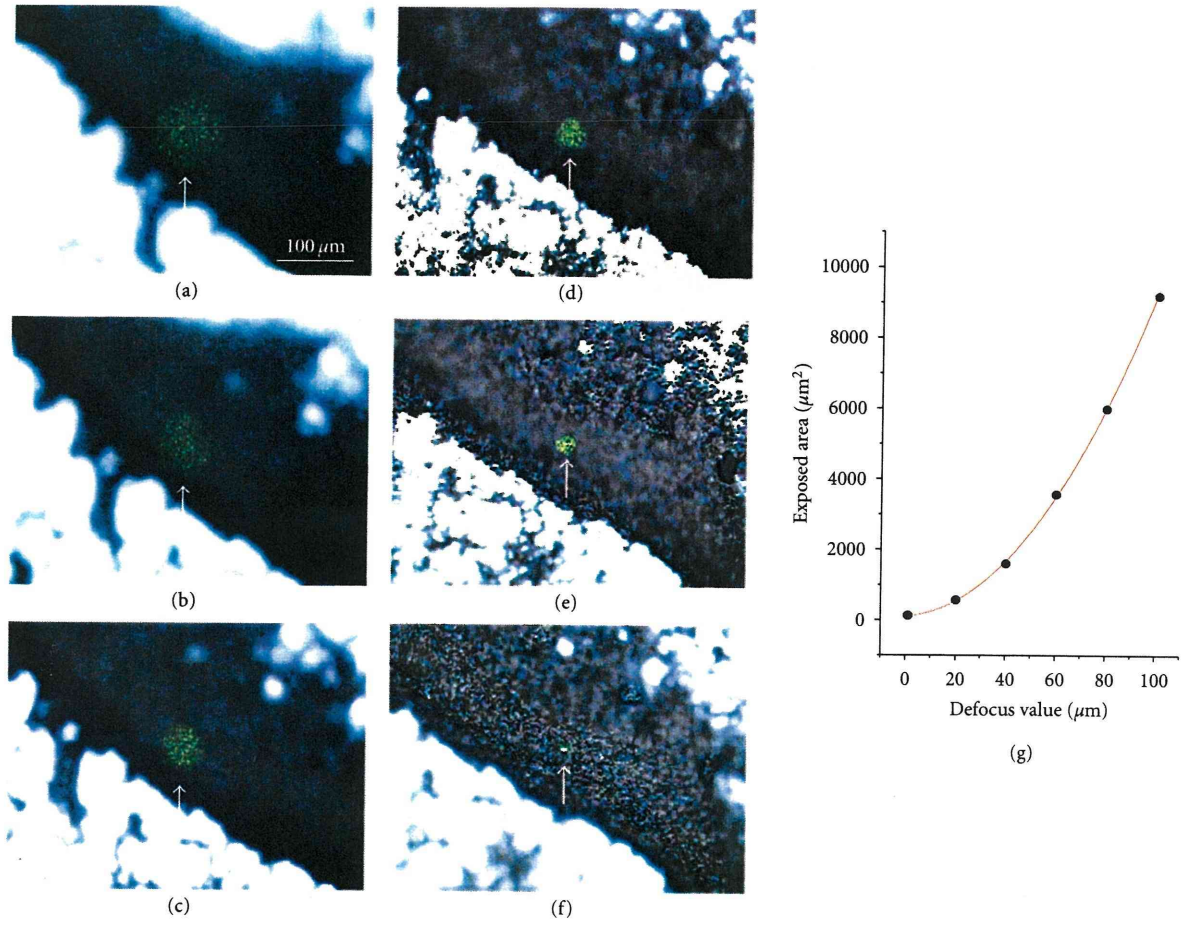

FIGURE 3: Optical microscopy images of the samples of C_{60}NWs irradiated by the excitation laser beams for the defocus values (under focus) of (a) 100, (b) 80, (c) 60, (d) 40, (e) 20, and (f) 0 μm and for the arrowed exposed areas of (a) 9270, (b) 6630, (c) 3480, (d) 1470, (e) 617, and (f) 63.8 μm^2, respectively. Graph (g) shows the relationship between the defocus value and the exposed area.

between OD1 and OD3. The ND filters OD1 (attenuation rate 0.1), OD2 (0.01), and OD3 (0.001) were used in the experiment, since the other filters gave too strong or too weak laser beam energies. The excitation laser beam power density could be varied from about 0.53 to 11800 mW/mm^2 using the above ND filters and by controlling the irradiation area of the laser beams and the defocus value from 0 to 100 μm as shown in **Figure 3**. The defocus value is defined as the distance from actual image plane and was set to be positive as the distance between the objective lens and the sample surface decreased. The places of C_{60}NWs exposed to the excitation laser beams can be recognized as the green circular areas marked in Figures 3(a)–3(f). The area of laser beam on the samples could be changed from 63.8 to 9270 μm^2 by controlling the defocus value from 0 to 100 μm.

The exposed area (y, μm^2) and the defocus value (x, μm) were plotted as shown in **Figure 3**(g). The plotted points can be approximated by the fitted quadratic curve, $y = 0.88x^2 + 6.8x + 36$. **Figure 4** summarizes the relationship among the laser beam power density, ND filter number, and the defocus value.

Figure 5 shows examples of the Raman spectra of C_{60}NWs taken by using the ND filters of OD1, OD2, and OD3 for an exposure time of about 220 s, where the spot size of laser beam on samples was 9 μm in diameter. Each power density of the excitation laser beam was (a) 11800, (b) 1660, and (c) 71.5 mW/mm^2, respectively. The $A_g(2)$ peak around 1468 cm^{-1} sifted to the lower wavenumbers with increasing the laser beam power density.

Figure 6 shows the $A_g(2)$ peak positions of the Raman spectra of C_{60}NWs as a function of energy dose of the laser beam for each defocus value from 100 μm to 0 μm (just focus). The power density of laser beam on samples was changed by changing the defocus value and the ND filter number as shown in **Figure 4**. The energy dose was changed by setting the beam exposure time at 215 ± 6 s, 441 ± 10 s, 665 ± 9 s, and 899 ± 29 s for each power density. Hence, as a whole, 72 data points are plotted in **Figure 6**. As shown in **Figure 5**, the Raman shifts are found to generally decrease to the lower values with increasing the energy dose. However, the Raman shifts were observed to increase along

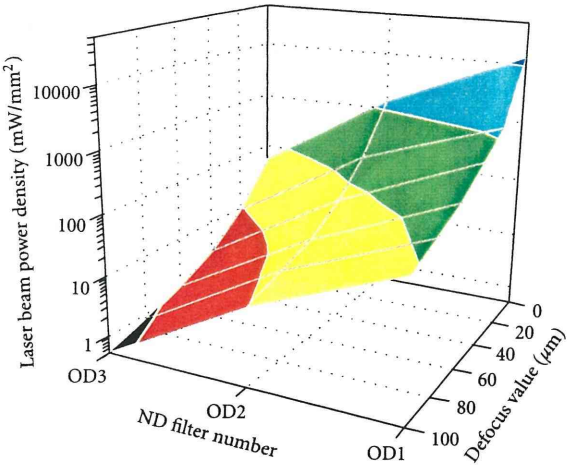

FIGURE 4: Power density of the Raman excitation laser beam measured as a function of ND filter number and the defocus value.

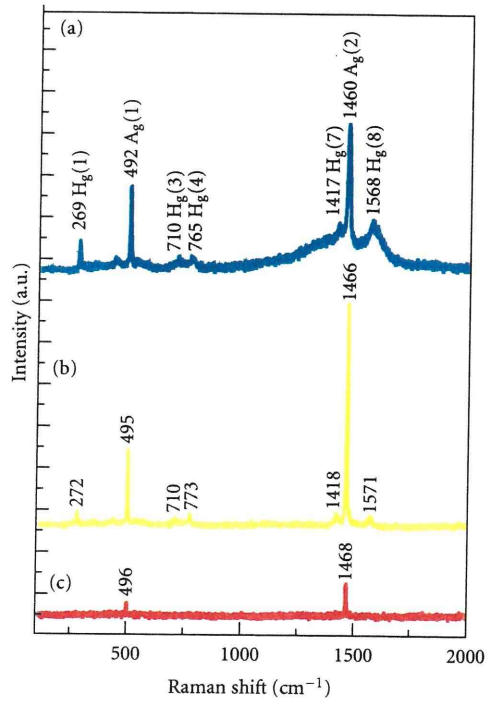

FIGURE 5: Raman spectra of C_{60}NWs. The power density of laser beam (D) is (a) 11800, (b) 1660, and (c) 71.5 mW/mm^2, respectively.

the red arrows for the high energy doses in Figures 6(c), 6(d), 6(e), and 6(f). These phenomena are supposed to be explained by the temperature rise of the C_{60}NWs exposed to the laser beams, since it is known that the photopolymerized C_{60} molecules decompose into their primary monomers and dimers by heating at temperatures higher than about 100°C [13].

The data points obtained using the highest power densities are indicated in each graph of Figure 6 by the black arrows for the exposure time of about 220 s. Figure 7 shows the relationship between the laser beam energy dose and the $A_g(2)$ peak position for the arrowed data points of Figure 6. The fitted curve of semilog plot is expressed as $y = -2.2x + 1467$, where x represents $\log_{10}$ (laser beam energy dose) and y represents the Raman shift of $A_g(2)$ peak. Using this experimental formula, the energy dose more than about 1520 J/mm^2 is found to be necessary for the photopolymerization of C_{60}NWs in air, when the laser light with a wavelength of 532 nm is used.

Since it is known that the photopolymerization of C_{60} progresses through the formation of four-membered rings between adjacent C_{60} molecules [11], it is considered that